Simpson, Angus Ross; Bergant, Anton Numerical comparison of pipe-column-separation models
Journal of Hydraulic Engineering, 1994; 120 (3):361-377

http://hdl.handle.net/2440/80915

NUMERICAL COMPARISON OF
PIPE-COLUMN-SEPARATION MODELS

Angus R. Simpson, Member, ASCE, and Anton Bergant

ABSTRACT: Results comparing six column-separation numerical models for simulating localized vapor cavities and distributed vaporous cavitation in pipelines are presented. The discrete vapor-cavity model (DVCM) is shown to be quite sensitive to selected input parameters. For short pipeline systems, the maximum pressure rise following column separation can vary markedly for small changes in wave speed, friction factor, diameter, initial velocity, length of pipe, or pipe slope. Of the six numerical models, three perform consistently over a broad number of reaches. One of them, the discrete gas-cavity model, is recommended for general use as it is least sensitive to input parameters or to the selected discretization of the pipeline. Three models provide inconsistent estimates of the maximum pressure rise as the number of reaches is increased; however, these models do give consistent results provided the ratio of maximum cavity size to reach volume is kept below 10%.

INTRODUCTION

The discrete vapor-cavity model (DVCM) for simulating transient events in pipelines involving water column separation is used in most commercial software packages for water-hammer analysis (Safwat et al. 1986). Since the introduction of the DVCM by Streeter (1969), the problems associated with multicavity collapse and their effect in producing unrealistic pressure spikes have been documented in the literature (Kranenburg 1974; Wylie and Streeter 1978a, b, 1993; Wylie 1984; Safwat et al. 1986; Simpson 1986; Golia and Greco 1990). In an effort to improve the performance of the DVCM, a number of variations of the model have been introduced (Safwat and van der Polder 1973; Kot and Youngdahl 1978; Miwa et al. 1990). As an alternative to the discrete vapor-cavity model, Provoost and Wylie (1981) introduced the discrete gas-cavity model (DGCM).

The primary objective of this paper is to compare the performance of various column-separation models. Detailed results from the discrete vapour-cavity models for two different reservoir-pipeline systems are presented. A comparison is made of the consistency of each column-separation model as the number of reaches (i.e., Δx and Δt) is systematically varied. The reach length Δx is used to discretize the pipeline, and Δt is the time step. In addition, the sensitivity of predicted peak pressures from the DVCM (staggered grid) to changes of input parameters (wave speed, friction factor, initial velocity, pipe diameter, length, and pipe slope) is investigated.

A finite difference scheme is convergent if the solution u tends to the exact solution U of the partial differential equations as both Δx and Δt tend to zero (Chaudhry 1987). Thus the numerical accuracy of column-separation models would be expected to improve as more reaches are used for the simulation as Δx and Δt become smaller and smaller. Previously, Provoost (1976) asserted that oscillations or unrealistic pressure spikes may be reduced by increasing the number of grid points in DVCM-type models. The results presented in this paper show that this is not necessarily the case, especially for the discrete vapor-cavity model. Instead of converging on a solution, the pressure-vs-time results diverge markedly as the number of reaches are increased. The cause of the large unrealistic pressures as predicted by DVCM-type numerical models has been identified as multi-cavity collapse of vapor cavities during column separation.

The partial differential equations for transient liquid flow in pipelines usually assume a constant wave speed of a. These equations are not valid for transient vaporous cavitating flow because pressure waves do not propagate at the wave speed a in these zones. Additionally, when a vaporous cavitation zone is condensed back to a liquid zone, the shock velocity (i.e., the rate at which vaporous mixture is converted to liquid) is highly variable but is always less than the liquid wave speed a. The DVCM is thus a simplistic approximation of the actual physical situation as a constant wave speed of a is assumed for both water-hammer and distributed vaporous-cavitation zones. Thus the DVCM converts the actual partial differential equations with a nonconstant wave speed (for the vaporous zones) to

different partial differential equations (with an assumed constant wave speed), then tries to correct for the error at the discrete vapor-cavity boundary(s).

DESCRIPTION OF MODELS
Water-Hammer Model

Unsteady flow in pipelines is described by one-dimensional equations of continuity and motion (Wylie and Streeter 1993):

$$H_t + VH_x - V\sin\theta + \frac{a^2}{g}V_x = 0 \tag{1}$$

$$V_t + VV_x + gH_x + \frac{fV|V|}{2D} = 0 \tag{2}$$

in which H = instantaneous piezometric head; V = instantaneous velocity of flow; θ = angle of pipe to horizontal; a = wave speed; g = gravitational acceleration; f = Darcy-Weisbach friction factor; and D = pipe diameter. Eqs. (1) and (2) are usually used in a simplified form by dropping the small slope and convective acceleration terms:

$$H_t + \frac{a^2}{gA}Q_x = 0 \tag{3}$$

$$Q_t + gAH_x + \frac{fQ|Q|}{2DA} = 0 \tag{4}$$

in which A = pipe area; and discharge Q is used instead of flow velocity V. The method of characteristics (Chaudhry 1987; Wylie and Streeter 1993) is a standard method for solving the unsteady-flow equations. Water-hammer compatibility equations valid along the positive characteristic C^+ *(dx/dt = a,* in which x = distance along the pipe and t = time) and the negative characteristic C^- *(dx/dt = -a)* for the liquid flow are:

$$H = C_P - B_P Q_u \tag{5}$$

$$H = C_m + B_m Q \tag{6}$$

in which Q_u = upstream discharge; Q = downstream discharge (both at the same computational section); and B_P, B_m C_P, and C_m = constants of water-hammer compatibility equations. The unconditionally stable linear implicit approximation of the friction term has been used (Wylie 1983; Chaudhry and Holloway 1984; Holloway and Chaudhry 1985). Wylie and Streeter (1993) obtained an expression for the friction term along the positive characteristic between points A and P using integration by parts as:

$$\int_{x_A}^{x_P} Q^2\, dx \approx Q_P|Q_A|(x_P - x_A) \tag{7}$$

Q_u, and Q at the same section in (5) and (6) are identical for the case of no column separation. At a boundary, the boundary equation replaces one of the compatibility equations.

Water-hammer equations for the liquid flow are valid when the pressure is above the liquid vapor pressure. If the pressure drops below the vapour pressure, column separation occurs either as a discrete cavity or a vaporous-cavitation zone (Simpson 1986; Simpson and Wylie 1991) in the liquid. The single-component one-phase flow is transformed into a single-component two-phase flow (liquid/liquid-vapor). Thus the standard water-hammer solution is no longer valid. The discrete vapor-cavity model (Wylie and Streeter 1978a, 1993) is the most widely used method to solve the described two-phase flow problem.

Streeter Model for Column Separation

The standard numerical algorithm for the discrete vapor-cavity model was developed by Streeter (1969). The model allows vapor cavities to form at computing sections in the method of characteristics. In implementing Streeter's model in this paper, the normal rectangular grid of the method of specified time intervals is applied to the simplified water-hammer compatibility equations, (5) and (6). A constant wave speed for the liquid between computational sections is assumed. When the pressure at a computational section drops below the vapor pressure of the liquid, it is set to the vapour pressure and a vapor cavity is assumed to occur. The standard water-hammer solution is no longer valid at the section. The discrete vapor cavity is fully described by two water-hammer compatibility equations; (5) and (6), with $H = H_v$, where H_v = vapor-pressure head. The discharge upstream Q_u. and downstream Q from the section can be obtained from (5) and (6). The continuity equation for the vapor-cavity volume is:

$$\Delta \forall_v = \int_{t_i}^{t_f} (Q - Q_u) \, dt \tag{8}$$

in which $\forall_v$ = vapor-cavity volume; t_i = initial time; and t_f = final time. The solution of the continuity equation for the vapor-cavity volume (Wylie 1984) is:

$$(\forall_v)_{t_f} = (\forall_v)_{t_i} + \left\{ (1 - \psi) \left[Q_{t_i} - (Q_u)_{t_i} \right] + \psi \left[Q_{t_f} - (Q_u)_{t_f} \right] \right\} (t_f - t_i) \tag{9}$$

where the subscript g on the $\forall$ terms has been replaced by v. Eq. (9) integrates the continuity equation for the volume of the vapor cavity using a weighting factor ψ in the time direction. The standard form of (9) uses a ψ value of 0.5 (Tanahashi and Kasahara 1969, 1970; Streeter 1972; Wylie and Streeter 1978a; Safwat et al. 1986); however, the weighting factor ψ can take on values between 0 and 1.0 although a practical range is 0.5-1.0.

The time step in the rectangular grid is based on the Courant condition for the characteristic lines:

$$t_f - t_i = \Delta t = \frac{\Delta x}{a} \tag{10}$$

When the cavity collapses at a section (as a result of a negative cavity volume), the one-phase liquid flow is reestablished and (5) and (6) are valid.

Discrete Vapor-Cavity Model

Two grids have been previously used in applying the method of characteristics: the normal rectangular grid and the staggered (or Evangelisti) grid. Fig. 1 shows that the normal rectangular grid is actually comprised of two independent staggered grids. The superposition of the waves may open two cavities in the two independent grids at the same time (P_1 and P_2) when the normal rectangular grid is used. A single cavity is opened when the staggered grid is used (P_1)-
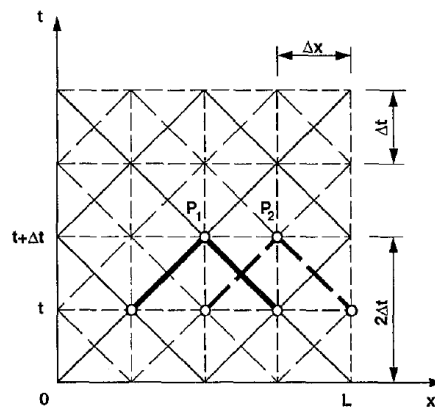

Figure 1.Staggered versus Rectangular Grid

Both the Streeter model and the DVCM (staggered grid) generate unrealistic pressure spikes due to pressure waves reflecting off cavities and end boundaries, and due to collapse of multicavities (Wylie and Streeter 1978b; Wylie 1984). To attempt to overcome this difficulty, several authors have used the discrete vapor-cavity model in a modified form.

All of the column-separation models investigated in this paper are derivatives of the discrete vapor-cavity model. Some of the corrections employed actually introduce numerical damping (e.g., Kot and Youngdahl 1978; Miwa et al. 1990). A correction based on interpolation must be regarded as somewhat arbitrary especially when we do not know how "unrealistic" the pressure peaks are and because the mechanisms of numerical attenuation are not fully understood.

Safwat and van der Polder Model
Safwat and van der Polder (1973) allowed discrete cavities to form only at predetermined locations (e.g., valve and high point). When pressure at the internal computational section drops below vapor pressure, the average discharge at this section $\bar{Q}$ is calculated from water-hammer compatibility equations, (5) and (6), with H set to H_v:

$$\bar{Q} = \frac{C_P B_m - C_m B_P + H_v B_P - H_v B_m}{2 B_P B_m} \tag{11}$$

Kot and Youngdahl Model
Kot and Youngdahl (1978) used the complete form of continuity [(1)] and the equation of motion [(2)]. Linear space-line interpolation was used within the normal rectangular grid in the method of characteristics. The compatibility water-hammer equations for this case are expressed as:

$$H = C_P + S - B_P Q_u \tag{12}$$

$$H = C_m + S + B_m Q \tag{13}$$

in which S = slope term constant. Interpolated discharges and heads are used for calculation of constants B_m, B_P, C_m, and C_P.

Miwa et al. Model
Miwa et al. (1990) modified Streeter's model by introducing artificial space-line interpolation. The interpolation is introduced by the equation:

$$\Delta t = 0.95 \frac{\Delta x}{a} \tag{14}$$

It is known that space-line interpolation causes numerical damping (Goldberg and Wylie 1983).

Discrete Gas-Cavity Model
As an alternative to the discrete vapor-cavity models, an application of a discrete gas-cavity model for analysis of vaporous cavitating flow has been introduced by Provoost and Wylie (1981) and Wylie (1984). A low gas void fraction $\alpha_g \leq 10^{-7}$ (the ratio between free-gas and free-gas-liquid mixture volume) should be selected. Discrete gas cavities replace discrete vapour cavities. Between each computing section, liquid is assumed to exist without free gas. The growth and diminishment of the gas cavity is calculated from the two water-hammer compatibility equations, (5) and (6), the continuity equation for the gas cavity [(9)] in which index g replaces v, and the equation of the ideal gas (isothermal process):

$$\forall g = \propto_O \forall \left(\frac{p_O^*}{p_g^*} \right) \tag{15}$$

in which $\forall_g$ = gas-cavity volume; $\propto_O$ = gas void fraction at a reference pressure; $\forall$ = mixture volume; p_O^* = absolute reference gas pressure; and p_g^* = absolute gas pressure.

The staggered grid has been used in this paper instead of the normal rectangular grid in the discrete gas-cavity model. For this case the time step is:

$$t_f - t_i = 2\Delta t = \frac{2\Delta x}{a} \tag{16}$$

METHODS FOR NUMERICAL COMPARISON OF MODELS
Convergence and Stability
The numerical solution used in each model in the form of finite difference approximations should satisfy both convergence and stability criteria (Smith 1978; Chaudhry and Holloway 1984; Chaudhry 1987). Convergence relates to behavior of the solution as Ax and At tend to zero while stability is concerned with round-off error growth (Chaudhry 1987). There are three approaches for the analysis of convergence or stability of finite difference approximations for the solution of the water-hammer equations: derivation of convergence or stability criteria for the nonlinear equations; derivation of criteria for linearized equations; and numerical solution of the equations for a number of different ~xs and Ats and examination of results (Collatz 1960; Maudsley 1984).

Previous studies of stability and accuracy of various solution schemes (interpolation, friction term integration) have used the third method (Wylie 1983; Chaudhry and Holloway 1984; Holloway and Chaudhry 1985; Chaudhry 1987). In this paper, the third method is also used to assess the performance of various column-separation models. The reach length 2~x is systematically increased to determine if the results converge.

RESULTS OF MODEL COMPARISONS
A comparison of column-separation models is made for a horizontal pipeline system with a valve at the downstream end (Fig. 2). The models are: DVCM, staggered grid; Streeter (1969) DVCM, rectangular grid; Safwat and van der Polder (1973); Kot and Youngdahl (1978); Miwa et al. (1990); and Provoost and Wylie (1981) DGCM.
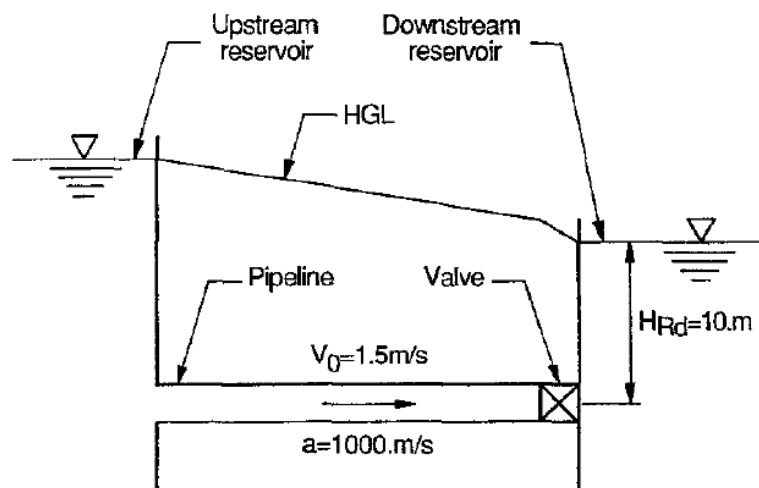

Figure 2. Pipeline System

A low head system was chosen because it is more sensitive to the occurrence of column separation and vaporous-cavitation zones during transients. Two cases including short and long pipes are considered (see Table 1). Short pipelines are often found in experimental laboratory setups, and longer pipelines are found in water-supply systems. A linear valve closure over a closure time t_c (Table 1) is used to initiate the transient in both pipelines. A steady-state velocity of $V_o = 1.5$ m/s was selected for all computer simulation runs.

Table 1. Data for Pipeline Systems

| Parameter (1)	Short pipe (2)	Long pipe (3)
Length, L (m)	50	5,000
Diameter, D (m)	0.2	1.2
Friction factor, f	0.026	0.017
Velocity V_O, (m/s)[a]	1.50	1.50
Valve-loss coefficient, K	0.35	0.35
Valve closure time, t_c (s)	0.0125	1.25
Simulation time, t_s (s)		400

[a]For all analyses presented.

Varying Number of Reaches in DVCM

A discrete vapor-capacity model including application of the staggered grid (SG) and integration of the cavity volume by (9) serves as a basic model (DVCM/SG) for numerical analysis. The influence of the different number of reaches (N = 4, 8, 16, 32, 64, 128, and 256; or ln N/ln2 = 2, 3, 4, 5, 6, 7, and 8, respectively) follows to compare the hydraulic grade lines (HGLs) predicted by the numerical model. The minimum HGL along the full length of both pipelines is equal to the liquid-vapor pressure head for all runs. The maximum cavity volume occurs at the valve and a distributed vaporous-cavitation zone is formed along the full length of the pipe for both systems. Results are presented for the maximum HGL at the valve, and the following parameters that characterize the transient event are investigated:

1. Ratio of maximum pressure head rise ΔH_{max} (= $H_{max} - H_o$) to the Joukowsky pressure head rise $a\Delta V/g$ shown in Fig. 3 (H_o = steady-state HGL at the valve).
2. Ratio of time occurrence of maximum pressure head t_{Hmax} to the pipe period L/a (Fig. 4).
3. Ratio of maximum cavity volume $\forall_{cav,max}$ to reach volume $\forall_{reach}$ (Fig. 5).
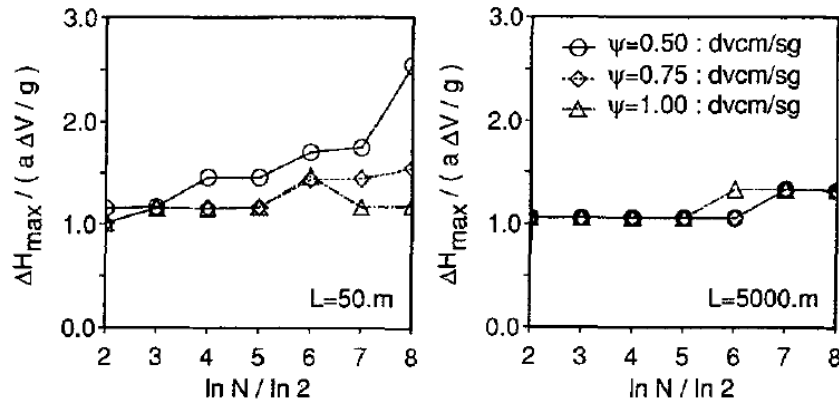
Figure 3. Ration of Maximum Pressure Rise to Joukowsky Pressure Rise at Valve
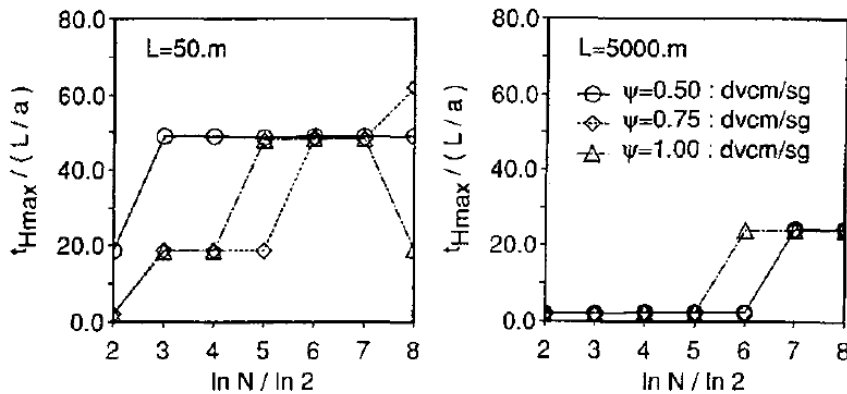
Figure 4. Ratio of Time of Occurrence of Maximum HGL at Valve to Pipe Period L/a
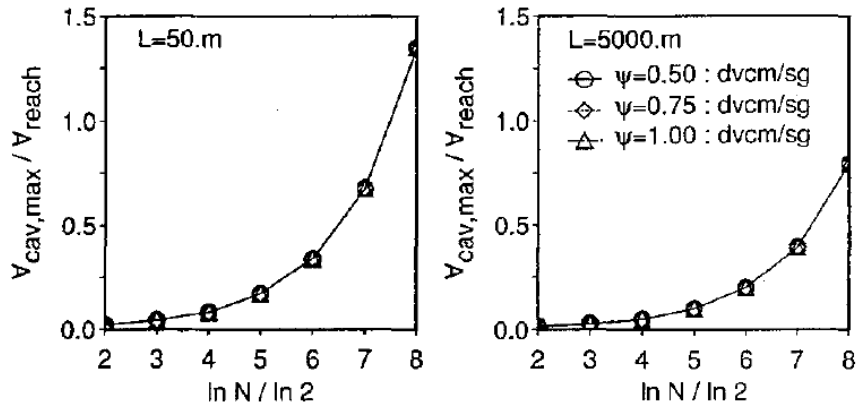
Figure 5.Ratio of Maximum Cavity Volume at Valve to Reach Volume

One conclusion from these results is that enough reaches should be selected to adequately model the valve closure, especially if column separation occurs. Fig. 3 shows a large deviation of the predicted maximum pressure for the short pipeline as the number of reaches is varied from four to 256. As the number of reaches increases to 32 (ln N/ln2 = 5) and above, there is considerable deviation and significant variation for different ψ values. For the long pipeline, the predicted maximum pressure rises are consistent for all ψ values up to 32 reaches. There is deviation in the predicted pressure rises for 64 reaches and above.

Fig. 4 shows the time of occurrence of the maximum pressure rise. For the short pipeline, it is clear that the time of occurrence of the maximum pressure rise varies considerably even for a low number of reaches. A detailed study of the formation and collapse of vapor cavities associated with the large pressure deviations was carried out. Waves due to cavity collapse were carefully traced on the *x-t* plane. The cause of the large unrealistic pressures is identified to be due to multicavity collapse. Depending on the number of reaches for the short pipeline, the maximum pressure in Fig. 4 occurs after the first-, second-, third-, or fourth-cavity collapse at the valve. For the long pipeline, friction plays a more important role. For N = 4 to N = 32, the time of maximum pressure rise is within 2L/a of the beginning of the valve closure. For 64 reaches (ln N/ln2 = 6) and above, the maximum pressure occurs well after the closure of the valve. The larger the number of reaches, the more cavities that form along the pipeline during column separation and the more chance of random multicavity collapse resulting in unrealistic superposition of waves.

Another important feature that should be considered is the size of the cavity at the valve. Fig. 5 shows that the maximum size of the cavity is consistent for all ψ values for both pipelines. The ratio of the maximum cavity volume at the valve to the reach volume increases as the number of reaches increases. The ratio is different for short and long pipelines for the same number of reaches. In formulating the discrete vapor-cavity model, an important assumption is the cavity volume is small compared with the reach volume. For the larger number of reaches in the two pipe cases considered, this assumption is violated.

For the short pipeline for N = 128 (ln N/ln2 = 7) and 256, the cavity volume at the valve exceeds 50% of the reach volume. This is unacceptable. A conclusion drawn from the results is that the maximum cavity volume should not exceed 10% of the reach volume. The basis for the 10% figure can be explained by considering Figs. 3-5. For the short pipeline the results for prediction of the maximum head in Figs. 3 and 4 are consistent for four, eight, and 16 reaches. The results deviate considerably for 32 reaches and above. In Fig. 5, the cavity volume at the valve for N = 16 (ln N/ln2 = 4) is 8.5% of the reach volume. For the long pipeline, the maximum pressure is equal to the Joukowsky pressure. For the long pipeline the numerical model results for prediction of the maximum head are consistent for N = four, eight, 16, and 32 reaches regardless Of the ψ value used. In Fig. 5 the cavity volume for 32 reaches is 10% of the reach volume.

Sensitivity of DVCM Results to Input Parameters

Another important feature of the numerical analysis is the sensitivity of the numerical model results to changes of input parameters. Several input parameters have been varied to assess sensitivity. These include wave speed a, friction factor f, initial velocity V_o, pipe diameter D, pipe length L, and pipe slope $(EL_d - EL_u)/L$, in which EL is pipeline elevation. The sensitivity analysis is now discussed for the case with N = 8 (ln$N$/ln2 = 3) and ψ = 1.0.

A variation of the wave speed of $\pm$ 10% (Fig. 6) resulted in a large scatter of the expected value of H_{max} at the valve for the short pipeline and no scatter for the long pipeline. An investigation of a friction factor for values in the range of f = 0-0.05 revealed an interesting physical behavior for both pipelines (Figs. 7 and 8). It appears that during transient cavitating flow the pipeline may operate in two regions depending on the size of the friction factor (or, indirectly on the velocity). Movement from one region to another occurs at a transition friction factor. For low friction factors the maximum pressure head is the short-duration pressure pulse (Simpson 1986) that follows after the cavity collapses (e.g., for f = 0.0324 in Fig. 7 and f = 0.0078 in Fig. 8). The Joukowsky pressure head is the maximum head for larger friction factors (e.g., for f = 0.0325 in Fig. 7 and f = 0.0079 in Fig. 8). Fig. 7 shows H_{max} at the valve for the short pipeline with a transition friction factor of f = 0.0324. The transition friction factor for the long pipeline is f = 0.0078 (Fig. 8). The variations of H_{max} for changes in diameter are shown in Fig. 9 (D = 0.1-0.3 m for the short pipeline and 1.0-1.4 m for the long pipeline). A transition occurs at a particular diameter. The transition is related to the resulting change in friction factor in a similar way as observed in Figs. 7 and 8. As the diameter increases, the friction factor decreases. Thus in Fig. 9 the maximum pressure to the left of the transition is governed by the Joukowsky pressure rise. To the right of the transition as the friction decreases the maximum pressure rise is determined by a short-duration pressure pulse following cavity collapse. Variation of pipe length of $\pm$ 4% for both pipelines (Fig. 10) leads to two transitions in the case of the short pipeline. Results for variation of pipe slope for both pipelines are shown in Fig. 11. For the short pipeline an increase in negative slope leads to more severe vaporous cavitation along the pipeline therefore decreasing the maximum pressure of the short-duration pulses.
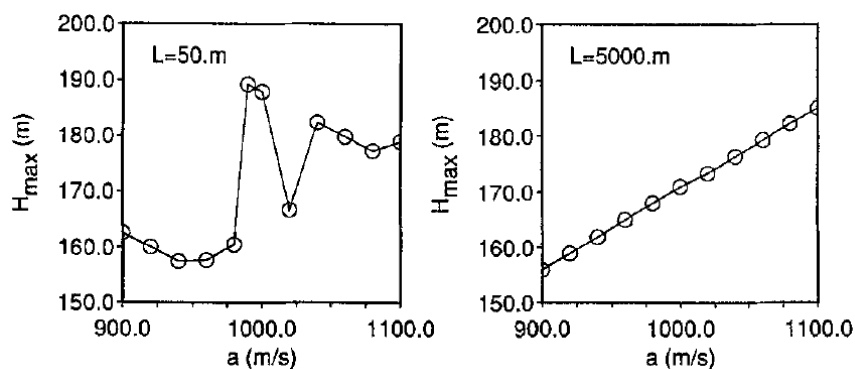

Figure 6. Maximum Head at Valve for Variable Wave Speed

Comparison of Column-Separation Models

A comparison of discrete vapor-cavity models using the normal rectangular grid is now considered for four models: Streeter (1990), Safwat and van der Polder (1973), Kot and Youngdahl (1978), and Miwa et al. (1990). Fig. 12 shows a large scatter of the maximum pressure head at the valve for the short pipeline as the number of reaches becomes large for the Streeter and Kot (unstable for N = 256) models. For the Safwat and the Miwa models, the predicted maximum pressure rises are consistent for all numbers of reaches. For the long pipeline, all the models give consistent results over the selected number of reaches (Fig. 12). The same type of behavior as for the maximum pressure head rise is observed for the time of occurrence of the maximum pressure rise at the valve (Fig. 13). The same conclusions as for the discrete vapor-cavity model using the staggered grid are drawn for the Streeter and Kot models (multicavity collapse). The Safwat model allows a discrete vapor cavity to form only at the valve; thus there is no multicavity collapse and subsequent unrealistic pressure spikes are
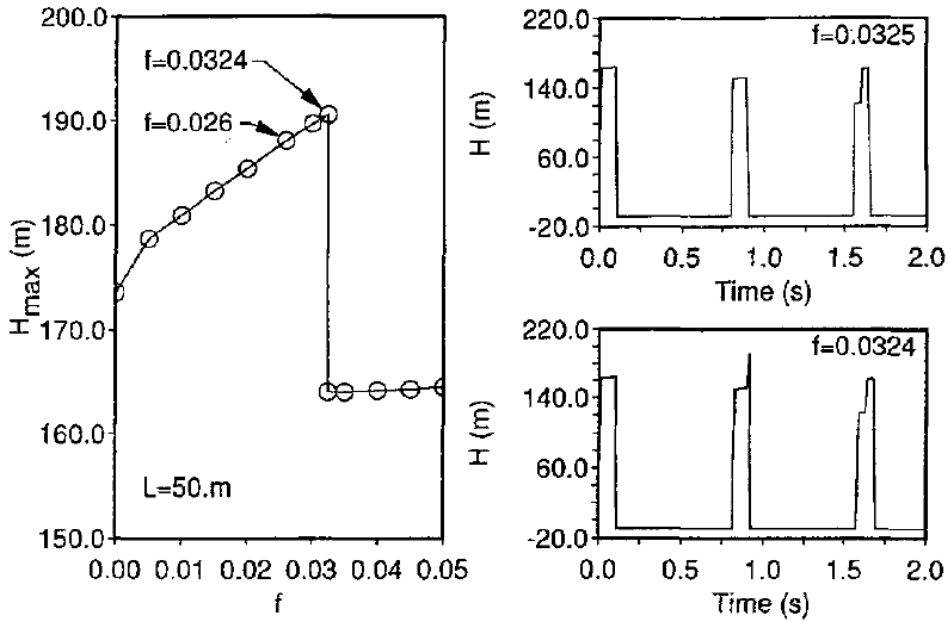
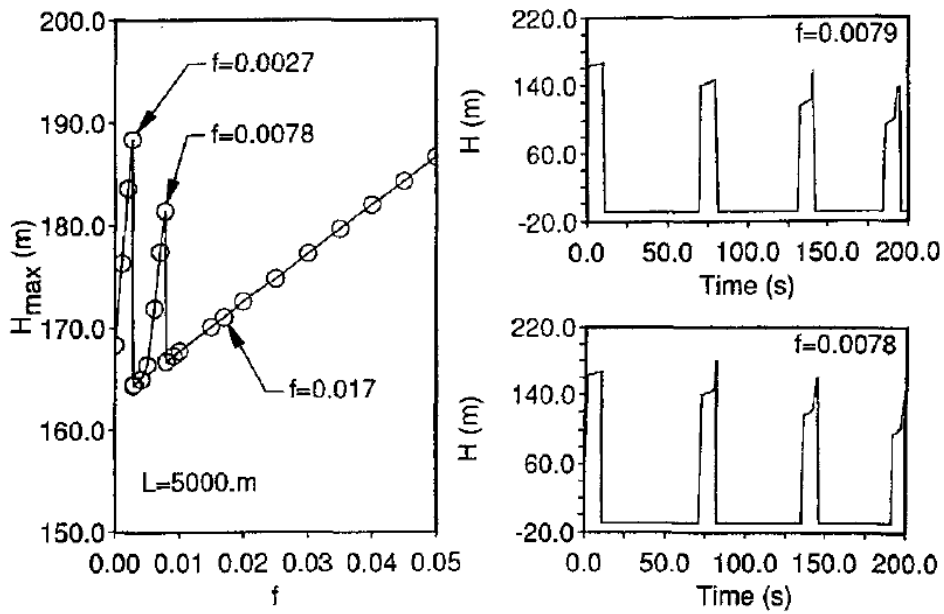**Figure 7. Maximum Head at Valve for Short Pipeline for Variable Friction Term**

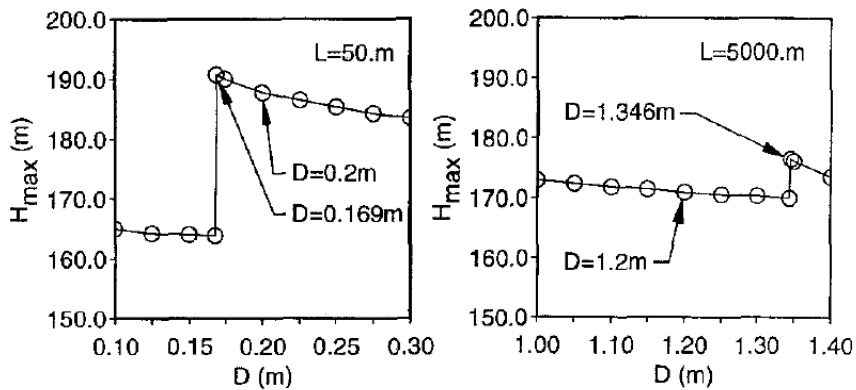**Figure 8. Maximum Head at Valve for Long Pipeline for Variable Friction Term**

Figure 9. Maximum Head at Valve for Variable Pipe Diameter
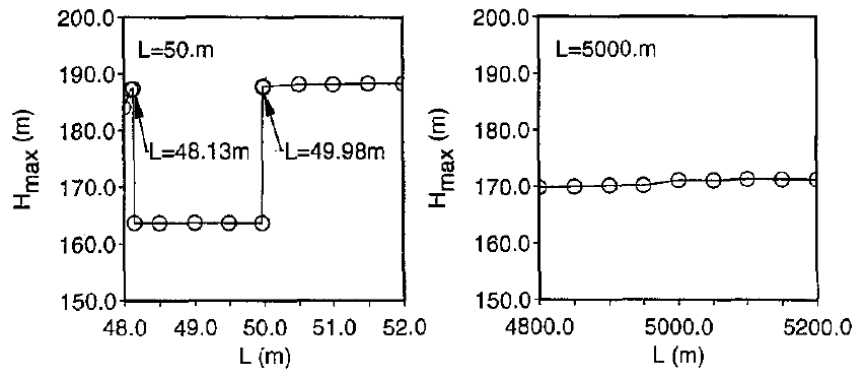
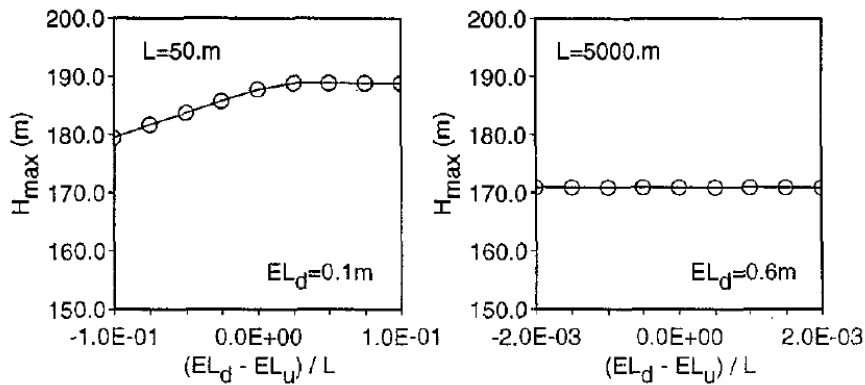**Figure 10. Maximum Head at Valve for Variable Pipe Length**

Figure 11. Maximum Head at Valve for Variable Pipe Slope

eliminated. Pressure pulses due to multicavity collapse in the Miwa model are significantly attenuated at interior computational sections, but this does not affect the maximum pressure head rise and the time of its occurrence. The analysis of the maximum size of the cavity at the valve (Fig. 14) shows that the increase of the cavity size predicted by the Miwa model is incorrect. With an increasing number of reaches, the size of the cavity is decreasing which is physically incorrect. An important conclusion for the Safwat model is that the ratio of maximum cavity volume at the valve to the reach volume does not affect the overall consistency of results. For the application of the Streeter and Kot model, the same conclusions as for the discrete vapor-cavity model using the staggered grid may be drawn (maximum cavity size should not exceed 10% of the reach volume).
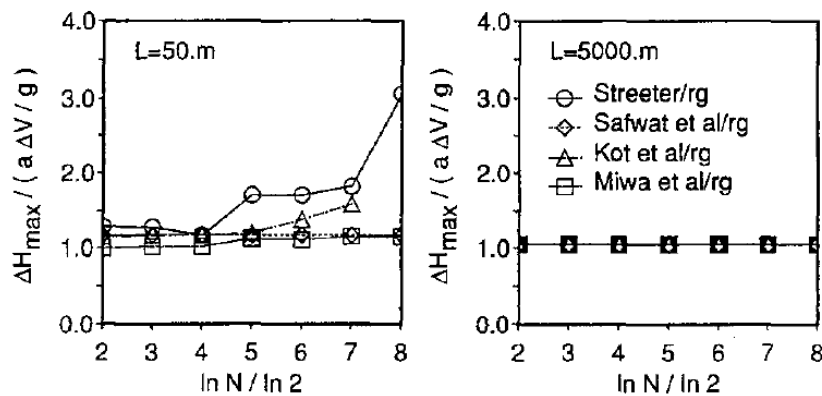

Figure 12. Ratio of Maximum Pressure Rise to Joukowsky Pressure Rise at Valve
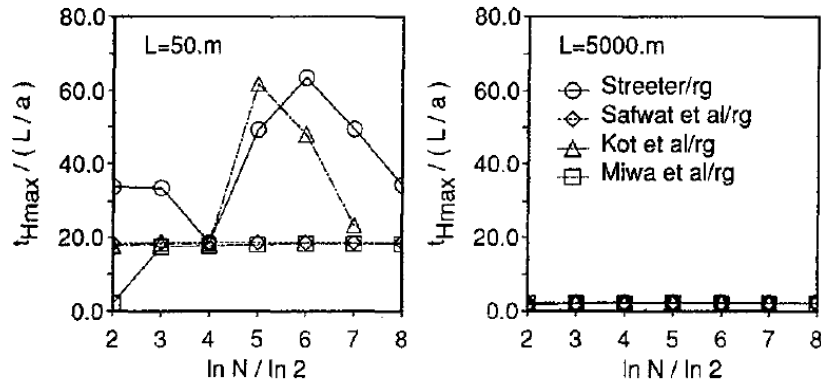
Figure 13. Ratio of Time Occurrence of Maximum HGL at Valve to Pipe Period *L/a*
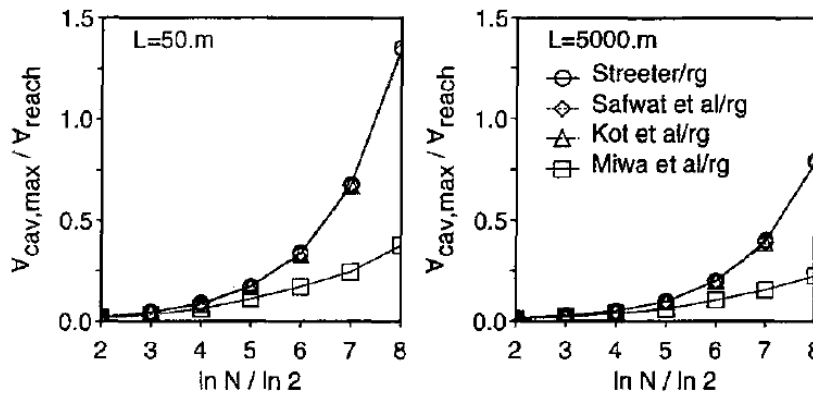

Figure 14. Ratio of Maximum Cavity Volume at Valve to Reach Volume

DGCM Results

Finally, the results for the discrete gas cavity model simulating transient vaporous cavitating flow ($\alpha_o = 10^{-7}$) are presented. As for DVCM enough reaches must be selected to adequately model the valve closure (Figs. 15 and 16). Figs. 15-17 show that predicted maximum pressure head rise at the valve, the time of occurrence of maximum pressure rise at the valve, and the maximum cavity volume at the valve are consistent for all numbers of reaches for both pipelines. The results from the DGCM are consistent even though the cavity volume exceeds the reach volume for the 256-reach case (for the short pipeline), as shown in Fig. 17. As for the Safwat and van der Polder model, the ratio of maximum cavity volume at the valve to the reach volume does not affect the overall consistency of the results (Fig. 17).
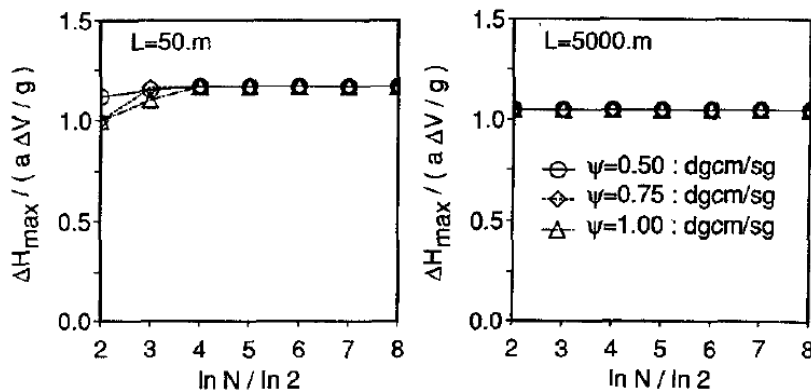

Figure 15. Ratio of Maximum Pressure Rise to Joukowsky Pressure Rise at Valve
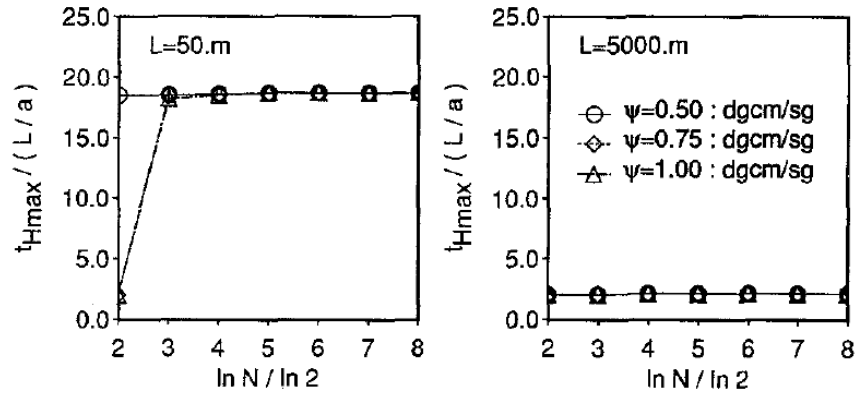
Figure 16. Ratio of Time of Occurrence of Maximum HGL at Valve to Pipe Period *L/a*
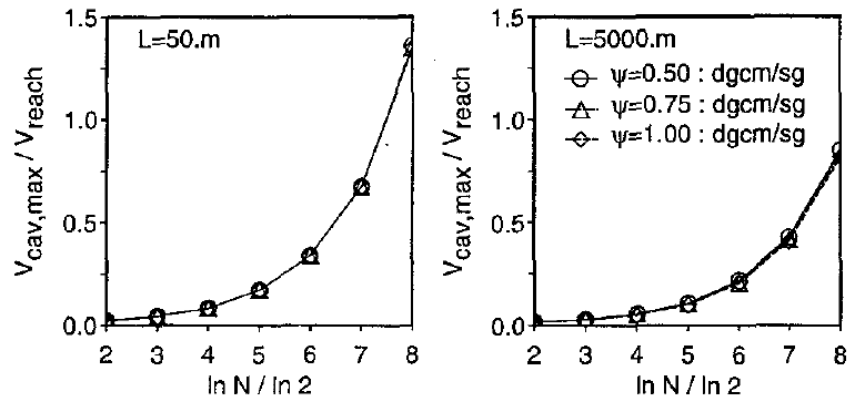

Figure 17. Ratio of Maximum Cavity Volume at Valve to Reach Volume

CONCLUSIONS

A comparison of five variations of the discrete vapor-cavity model has been presented. In addition the results from the discrete gas-cavity model are presented. Two pipeline systems including short pipelines and long pipelines have been studied. The sensitivity of results of maximum pressure head predicted by the discrete vapor-cavity model (staggered grid) to changes in parameters have also been presented. The recommended limits for application of the DVCM model described here have been taken into consideration in the sensitivity analysis. The maximum pressure can vary significantly particularly for short pipelines for small changes in wave speed, friction factor, initial steady-state pipe velocity, pipe diameter, or pipe slope. As part of a water-hammer study where column separation occurs, it is recommended that a sensitivity analysis should be performed to ensure the maximum pressure head is not being underestimated.

Multicavity collapse produces unrealistic pressure spikes, when the number of reaches becomes too large for the following models: the Streeter model, the Kot and Youngdahl model, and the discrete vapor-cavity model with a staggered grid. Care must be exercised when using any of these three models. The number of reaches should be chosen such that the ratio of the maximum size of any cavity volume to reach volume must be kept below about 10%. Thus the number of reaches must actually be restricted to ensure reasonably accurate predictions are obtained of the maximum pressure following column separation.

Three models gave consistent results for prediction of the maximum pressure head in both pipeline systems regardless of the number of reaches (from four to 256). These models were the Safwat and van der Polder model, the Miwa et al. model, and the discrete gas-cavity model. The Safwat and van der Polder model has only a single cavity at the valve and thus avoids problems due to multicavity collapse. A disadvantage is that the user has to preselect the potential locations where localized vapor cavities may form. The Miwa et al. model introduces numerical dampening due to space-line

interpolation and there may be circumstances where the results are incorrect. The vapor cavity volume at the valve is also incorrect for the Miwa et al. model.

The discrete gas-cavity model with a very small void fraction of air at the computational sections (α_o = 10^{-7}) performs accurately over a broad range of numbers of reaches. The use of DGCM is recommended for modeling column separation, rather than the DVCM or one of its variations. However, care must be exercised even when using the DGCM. The DGCM seems to behave consistently over a broad number of different reaches for the two examples considered in this paper; however, this does not mean the model is necessarily correct. Further investigation is required to determine whether other examples also provide consistent results. One way of avoiding the problem of reach selection in the DVCM-type model is to move to other types of models such as the distributed vaporous-cavitation model (Bergant and Simpson 1992), which is based on the separate modeling of different flow regions and tracking of interface movements.

APPENDIX I. REFERENCES
Bergant, A., and Simpson, A. R. (1992). "Interface model for transient cavitating flow in pipelines." *Unsteady flow and fluid transients,* R. Bettess and J. Watts, eds., A. A. Balkema, Rotterdam, The Netherlands, 333-342.

Chaudhry, M. H. (1987). *Applied hydraulic transients.* 2nd Ed., Van Nostrand Reinhold, New York, N.Y.

Chaudhry, M. H., and Holloway, M. B. (1984). "Stability of method of characteristics." *Proc. ASCE Hydr. Div. Specialty Conf.,* ASCE, 216-220.

Collatz, L. (1960). *The numerical treatment of differential equations.* 3rd Ed., Springer Verlag, Berlin, West Germany.

Goldberg, D. E., and Wylie, E. B. (1983). "Characteristics method using time-line interpolations." *J. Hydr. Engrg.,* ASCE, 109(5), 670-683.

Golia, U. M., Greco, M. (1990). "Cavitation during water-hammer: Quick closure of a downstream valve." *Hydrosoft '90, Proc. 3rd Int. Conf. on Hydr. Engrg. Software,* W. R. Blair and D. Quazar, eds., Lowell, Mass., 121-129.

Holloway, M. B., and Chaudhry, M. H. (1985). "Stability and accuracy of water hammer analysis." *Advances in Water Resour.,* 8, 121-128.

Kot, C. A., and Youngdahl, C. K. (1978). "Transient cavitating effects in fluid piping systems." *Nuclear Engrg. and Design,* 45(1), 93-100.

Kranenburg, C. (1974). "Gas release during transient cavitation in pipes." *J. Hydr. Div.,* ASCE, 100(10), 1383-1398.

Maudsley, D. (1984). "Errors in the simulation of pressure transients in a hydraulic system." *Trans.,* Institute of Measurement and Control, 6(1), 7-12.

Miwa, T., Sano, M., and Yamamoto, K. (1990). "Experimental studies on water hammer phenomenon including vapour column separation." *Water Supply,* 8(3- 4), 430-438.

Provoost, G. A. (1976). "Investigations into cavitation in a prototype pipeline caused by water hammer." *Proc. 2nd Int. Conf. on Pressure Surges,* British Hydromechanics Research Association, Cranfield, U.K., D2-12-D2-29.

Provoost, G. A., and Wylie, E. B. (1981). "Discrete gas model to represent distributed free gas in liquids." *Proc. 5th Int. Syrup. on Column Separation,* International Association of Hydraulic Research, The Netherlands, 249-258.

Safwat, H. H., and van tier Polder, J. (1973). "Experimental and analytic data correlation study of water column separation." *J. Fluids Engrg.,* 94(1), 91-97.

Safwat, H. H., Aratsu, A. H., and Husaini, S. M. (1986). "Generalized applications of the method of characteristics for the analysis of hydraulic transients involving empty sections." *Proc. 5th Int.*

Conf. on Pressure Surges, British Hydromechanics Research Association, Cranfield, U.K., 157-167.

Simpson, A. R. (1986). "Large water hammer pressures due to column separation in a sloping pipe," PhD thesis, University of Michigan, Ann Arbor, Mich.

Simpson, A. R., and Wylie, E. B. (1991). "Large water hammer pressures for column separation in pipelines." *J. Hydr. Engrg.,* ASCE, 117(10), 1310-1316.

Smith, G. D. (1978). *Numerical solution of partial differential equations.* 2nd Ed., Clarendon Press, Oxford, England.

Streeter, V. L. (1969). "Water hammer analysis." *J. Hydr. Div.,* ASCE, 95(6), 1959-1972.

Streeter, V. L. (1972). "Unsteady flow calculations by numerical methods." *J. Basic Engrg.,* 94(2), 457-466.

Tanahashi, T., and Kasahara, E. (1969). "Analysis of water hammer with column separation." *Bull. Japan Soc. of Mech. Engrs.,* Japan, 12(50), 206-214.

Tanahashi, T., and Kasahara, E. (1970). "Comparisons between experimental and theoretical results of the water hammer with water column separation." *Bull. Japan Soc. of Mech. Engrs.,* Japan, 13(61), 914-925.

Wylie, E. B. (1983). "The microcomputer and pipeline transients." *J. Hydr. Engrg.,* ASCE, 109(12), 1723-1739.

Wylie, E. B. (1984). "Simulation of vaporous and gaseous cavitation." *J. Fluids Engrg.,* 106(3), 307-311.

Wylie, E. B., and Streeter, V. L. (1978a). *Fluid transients.* McGraw-Hill, New York, N.Y.

Wylie, E. B., and Streeter, V. L. (1978b). "Column separation in horizontal pipelines." *Proc. Joint Syrup. on Design and Operation of Fluid Machinery,* ASCE, New York, N.Y., 1, 3-13.

Wylie, E. B., and Streeter, V. L. (1993). *Fluid transients in systems.* Prentice-Hall, Inc., Englewood Cliffs, N.J.

APPENDIX II. NOTATION

The following symbols are used in this paper:

A	=	pipe area
a	=	wave propagation velocity
B_m, B_P	=	known constants of water-hammer compatibility equations
C_m, C_P	=	known constants of water-hammer compatibility equations
D	=	diameter of pipe
EL_d	=	downstream pipeline elevation
EL_u	=	upstream pipe elevation
f	=	Darcy-Weisbach friction factor
g	=	gravitational acceleration
H	=	instantaneous piezometric head
H_{max}	=	maximum pressure head
H_o	=	steady state HGL at valve
H_{Rd}	=	downstream reservoir head
H_v	=	vapour pressure head
K	=	valve-loss coefficient
L	=	pipeline length
N	=	number of reaches in pipeline
p_g^*	=	absolute gas pressure
p_o^*	=	absolute reference gas pressure
Q	=	instantaneous discharge or downstream discharge at section
$\bar{Q}$	=	average discharge at section
Q_u	=	upstream discharge at section
R	=	resistance coefficient
S	=	pipe-slope term constant
t	=	time
t_c	=	closure time

t_f	=	final time
$t_{H\text{max}}$	=	time at maximum pressure
t_i	=	initial time
t_s	=	simulation time
U	=	exact solution of the partial differential equations
u	=	exact solution of the finite difference scheme
V	=	instantaneous velocity of flow
V_o	=	steady-state velocity of pipeline
x	=	distance
α_o	=	gas void fraction at reference pressure
α_g	=	gas void fraction
ΔH_{max}	=	maximum pressure head rise
Δt	=	time step
ΔV	=	velocity change
θ	=	angle of pipe to horizontal
ψ	=	weighting factor
$\forall$	=	mixture volume
$\forall_g$	=	gas-cavity volume
$\forall_v$	=	vapor-cavity volume
$\forall_{\text{cav,max}}$	=	maximum cavity volume
$\forall_{\text{reach}}$	=	reach volume